



UNIVERSITY OF LEEDS

This is a repository copy of *Simple technique for high-throughput marking of distinguishable*.

White Rose Research Online URL for this paper:  
<http://eprints.whiterose.ac.uk/92514/>

Version: Accepted Version

---

**Article:**

Henrichs, L, Chen, L and Bell, A (2016) Simple technique for high-throughput marking of distinguishable. *Journal of Microscopy*, 262 (1). pp. 28-32. ISSN 0022-2720

<https://doi.org/10.1111/jmi.12337>

---

**Reuse**

Unless indicated otherwise, fulltext items are protected by copyright with all rights reserved. The copyright exception in section 29 of the Copyright, Designs and Patents Act 1988 allows the making of a single copy solely for the purpose of non-commercial research or private study within the limits of fair dealing. The publisher or other rights-holder may allow further reproduction and re-use of this version - refer to the White Rose Research Online record for this item. Where records identify the publisher as the copyright holder, users can verify any specific terms of use on the publisher's website.

**Takedown**

If you consider content in White Rose Research Online to be in breach of UK law, please notify us by emailing [eprints@whiterose.ac.uk](mailto:eprints@whiterose.ac.uk) including the URL of the record and the reason for the withdrawal request.



[eprints@whiterose.ac.uk](mailto:eprints@whiterose.ac.uk)  
<https://eprints.whiterose.ac.uk/>

## Simple technique for high-throughput marking of distinguishable micro-areas for microscopy

Leonard F. Henrichs<sup>1,\*</sup>, Li Chen<sup>2</sup>, and Andrew J. Bell<sup>1</sup>

<sup>1</sup>University of Leeds, Institute for Materials Research, Engineering Building, LS2 9JT  
Leeds, United Kingdom

<sup>2</sup>University of Leeds, School of Electronic and Electrical Engineering, LS2 9JT  
Leeds, United Kingdom

### Abstract

Today's (nano)-functional materials, usually exhibiting complex physical properties require local investigation with different microscopy techniques covering different physical aspects such as dipolar and magnetic structure. However, often these must be employed on the very same sample position to be able to truly correlate those different information and corresponding properties. This can be very challenging if not impossible especially when samples lack prominent features for orientation.

Here, we present a simple but effective method to mark hundreds of approx.

15x15  $\mu\text{m}$  sample areas at one time by using a commercial TEM grid as shadow mask in combination with thin-film deposition. Areas can be easily distinguished when using a reference or finder grid structure as shadow mask. We show that the method is suitable to combine many techniques such as light microscopy, scanning probe microscopy and scanning electron microscopy. Furthermore, we find that best results are achieved when depositing aluminium on a flat sample surface using electron-beam evaporation which ensures good line-of-sight deposition. This inexpensive high-throughput method has several advantages over other marking techniques such as focused ion-beam (FIB) processing especially when batch

processing or marking of many areas is required. Nevertheless, the technique could be particularly valuable, when used in junction with e.g. FIB sectioning to obtain a thin lamellar of a particular pre-selected area.

## Introduction

As modern materials such as functional oxides, semiconductors or biomaterials become more and more complex, but also smaller and smaller (Drexler, 1992), it becomes necessary to study their multiple properties with different microscopy techniques. These can provide information on, for example, local composition, crystal structure, mechanical properties, magnetic and dipolar order (Rodriguez *et al.*, 2009). Areas of material's research where it is important to acquire these local data are in multiferroics, Li-ion battery, fuel cell materials and graphene (Fiebig, 2005, Goodenough & Park, 2013, Geim & Novoselov, 2007). Today, there exist a multitude of microscopy techniques which are able to measure numerous different properties with high spatial resolution. Among the most prominent examples are scanning force microscopy, (Binnig *et al.*, 1986, Giessibl, 2003) electron microscopy (Vernon-Parry, 2000) and confocal laser scanning microscopy (Amos & White, 2003) for all of which, numerous sub-techniques have been developed. However, it is often necessary to use these different techniques on the very same sample area in order to correlate the corresponding properties with each other. This can be challenging if not impossible without marking techniques, given the fact that the local information are obtained on areas that are often not larger than  $10 \times 10 \mu\text{m}$ .

Here we present a convenient, quick and inexpensive way to mark many areas at the same time on one sample, for the purpose of revisiting the very same area with different microscopy techniques. The technique can be utilized to mark areas on

samples that do not exhibit prominent features for orientation. Furthermore, it is less expensive and time consuming than marking of sample areas e.g. by FIB (Sanborn & Myers, 1991) and it allows marking of many areas on many samples with just one thin-film deposition which makes it particularly interesting for batch processing.

For marking, commercial copper grids for transmission electron microscopy (TEM) (without a support film) in combination with thin-film deposition are used to mark more than 500 areas on a sample at one time. More precisely, a TEM grid is first put on top of the samples surface to act as a shadow mask for a metal thin-film which leaves open areas on the sample surface that are connected in a cross shape manner, and coated square shaped areas. The uncoated areas which usually have sizes of approx.  $15 \times 15 \mu\text{m}$  can be used for imaging. Fig. 1a-c illustrates the principle of this method schematically.

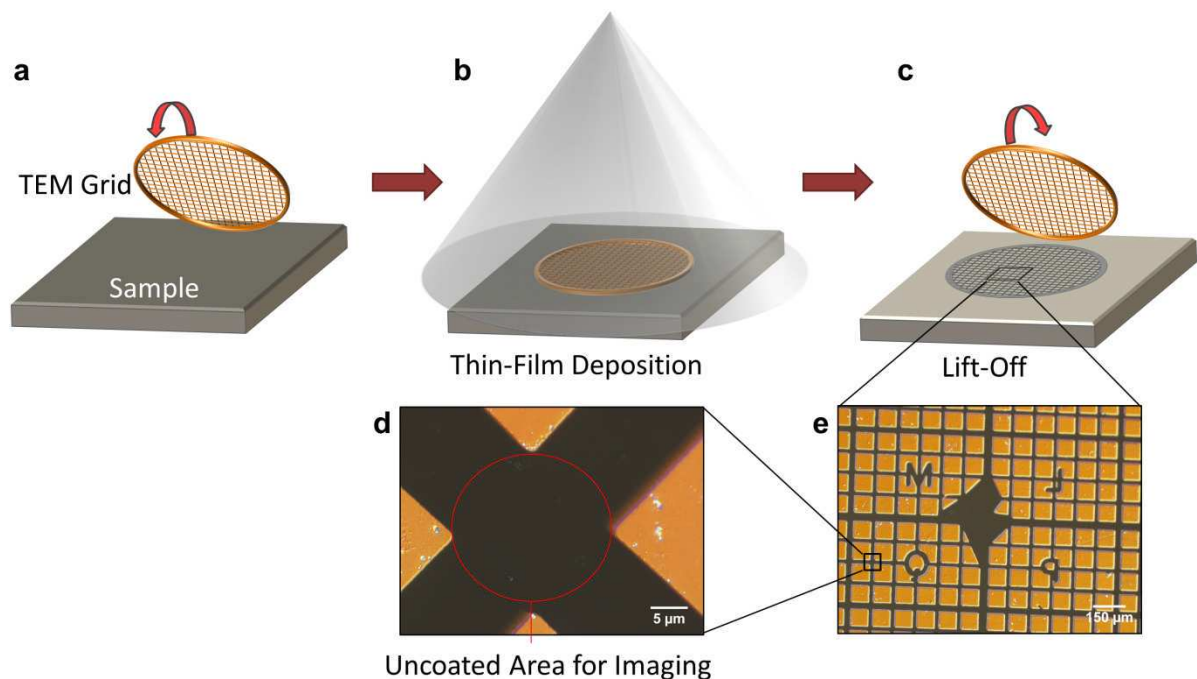


**Figure 1 Schematic illustration of the principle of the marking technique.** The marking technique involves three steps: **a**, Applying TEM grid to flat sample surface. **b**, Deposition of thin-film. **c**, Lift-off

of TEM grid from sample surface, leaving uncoated sample area in shape of the TEM grid. **e**, Light microscopy image showing finder structure on glass slide (note colours are false due to differential interference contrast DIC used for imaging). **d**, Magnification of cross shaped uncoated area. Imaging can be carried out e.g. in the centre of the cross shaped open sample areas. These can be made distinguishable by using an appropriate TEM grid with finder structure (i.e. letters).

TEM grids with appropriate finder structure (letters) enable discrimination of different sample areas e.g. with conventional light microscopy (see Fig. 1d,e). These grids are inexpensive and can be bought in large quantities, which allows single use of each TEM grid. Fig. 1e shows a cross-shaped uncoated area in high magnification which can be used for imaging.

Below we will show how this technique can be employed to investigate the same sample area with scanning probe microscopy and scanning electron microscopy (SEM). In particular, we used piezoresponse force microscopy (PFM) (Soergel, 2011, Henrichs *et al.*, 2015) and SEM with energy dispersive X-ray spectroscopy (EDX) to image both the dipolar order (ferroelectric domain pattern) and the chemical composition of the same area. However, the technique can be used for any other microscopy technique, with the only prerequisite that the coated and uncoated areas need to be distinguishable with the corresponding technique.

## Experimental

Polycrystalline  $(\text{BiFeO}_3)_{0.65}-(\text{PbTiO}_3)_{0.35}$  ferroelectric ceramics, which were prepared via a conventional solid state reaction route, (Comyn *et al.*, 2004) were first polished on a Motopol 2000 ( Buehler, Lake Bluff, Illinois, USA) in several steps using various polishing-cloths in combination with diamond abrasive-liquids (both by Buehler) where the diamond particle-size was gradually reduced for consecutive steps, until  $1 \mu\text{m}$  particles were reached. The final surface roughness was in the range of ten nanometres. A commercial TEM grid (Maxtaform Reference Finder Grids, Style H7,

400 mesh, Copper, Ted Pella, Redding, California, USA) was clamped on the surface of each polished sample which were then attached to a sample holder. The whole assembly was loaded into the process chamber of an electron beam evaporator LeyboldUnivex 350 system (Oerlikon Leybold Vacuum, Cologne, Germany) with sample to source distance 375 mm. After a vacuum lower than  $1 \times 10^{-6}$  mBar had been reached, the aluminium source was melted by an electron beam. Thin-film deposition and thickness (approx. 60 nm) were controlled by an automated shutter system in combination with a quartz crystal microbalance.

AFM respectively PFM experiments were carried out on a 5420 AFM by Agilent Technologies (Santa Clara, California, USA) equipped with the MAC Mode III extension; DCP11 conductive-diamond coated tips by NT-MDT (Moscow, Russia) were used.

SEM imaging was carried out in back-scatter electron (BSE) imaging mode with 20 kV acceleration voltage on an EVO MA15 by Carl Zeiss (Oberkochen, Germany) equipped with AZtecEnergy EDX system (Oxford Instruments, Abingdon, United Kingdom).

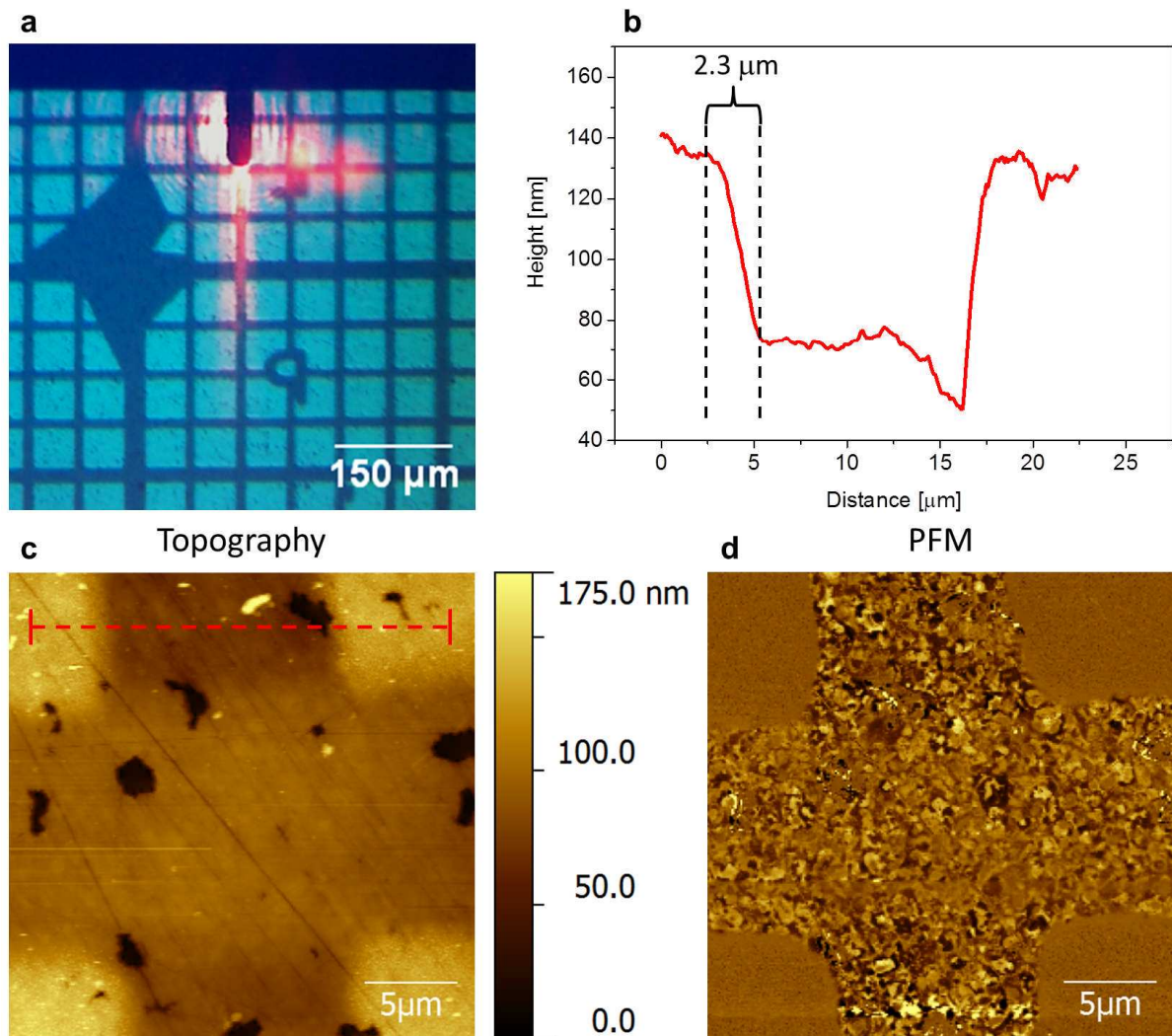
## Results

For deposition of the film, we found that a flat sample surface is very important to ensure that gaps between grid and sample surface are minimized. If the grid does not lie flat but is some distance away from the surface, this results in formation of a shadow from the aluminium source to the sample surface. As a result, there exists a grey area between the fully exposed and fully obscured area, which leads to undefined and broad edges between coated and uncoated areas, which is undesirable.

Two different deposition techniques, electron-beam evaporation and sputter-coating with argon plasma, were tested. As expected, we found that edges were narrower for electron-beam evaporation due to the deposition being almost exclusively in line-of-sight. In contrast, sputter-coating causes more diffuse deposition and thus edges become broader and blurry although marking is still possible.

Furthermore, several thin-film materials were tested and the best results, in terms of mechanical stability, were achieved for aluminium films. In case of a softer gold film, problems were encountered for AFM imaging. In contact imaging mode which is used for PFM, the film was damaged while the tip was scanned across it, which resulted in stripe-like imaging artifacts presumably due to the “smearing” of gold particles across the surface during scanning. However, this was not the case for the aluminium film presumably due to the much harder aluminium oxide layer on the surface.

Fig. 2 shows how the technique is employed to image a specific sample area with AFM.



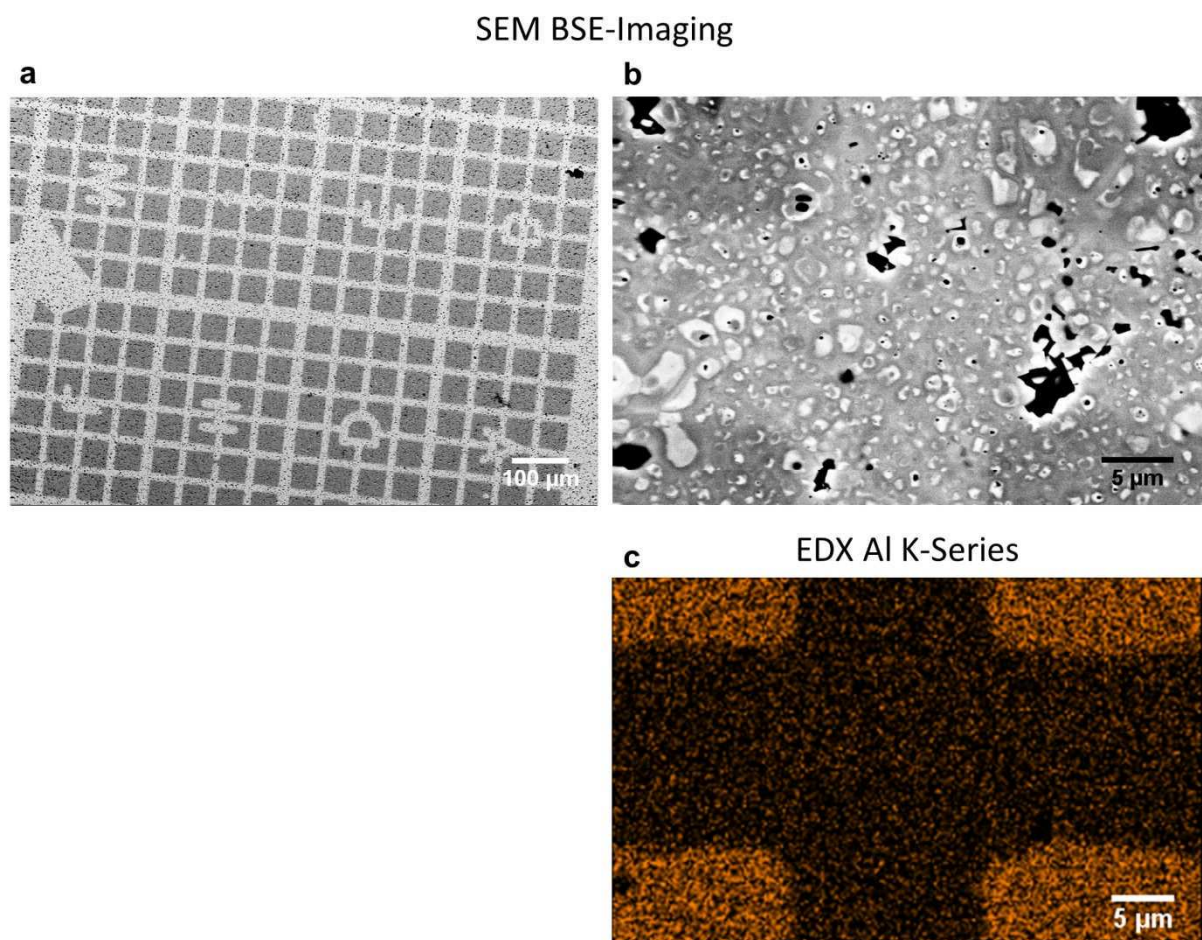
**Figure 2 Finding specific sample area with AFM/PFM.** **a**, Micrograph taken with the light microscope integrated in the AFM. The cantilever with laser spot reflected from the back side is visible at the top middle, with the AFM tip situated underneath the bottom end of the cantilever. **b**, Cross section through topography according to red dashed line in **c**. The width of the film edge is approx. 2.3 μm. **c,d**, Topography and corresponding PFM image (X-channel or mixed signal) of cross shaped uncoated area respectively. Note that PFM contrast is only seen in the uncoated areas.

Fig. 2a shows how the finder structure can be used to move the AFM tip to the desired free sample area, using an integrated light microscope with low magnification. In our case, we used a simple X-Y-stage which was operated by hand using two screws, for moving the sample relative to the tip. Fig. 2c and d show topography and PFM images (X-channel or mixed signal) respectively of a cross shaped open sample area. Note that in coated areas (bright in topography) there is no PFM signal whereas in the uncoated area, the ferroelectric domain pattern of the



ceramic  $(\text{BiFeO}_3)_{0.65}-(\text{PbTiO}_3)_{0.35}$  sample is visible. The low width of the thin-film edge ( $2.3 \mu\text{m}$ ) which is visible in the topography cross-section according to the red dashed line in Fig. 2c, allows accurate localisation of sample areas. The film thickness was approx.  $60 \text{ nm}$  as visible in Fig. 2b.

The same localization procedure was also tested for SEM with EDX which is shown in Fig. 3.



**Figure 3 Finding specific sample area with SEM and EDX.** **a**, SEM backscattered electron (BSE) image of larger area showing the finder structure on the sample surface. **b**, Zoomed SEM BSE image of an area suitable for imaging. **c**, Map of EDX Al-K series of the same area as in **b** showing the elemental distribution of aluminium in this area. As expected, aluminium is found only in coated areas.

Fig. 3a shows how coated and uncoated area can be easily distinguished by SEM using backscattered electron (BSE) imaging mode which has an atomic number contrast (z-contrast). Note that in conventional secondary electron imaging, a thin

aluminium film is usually not visible. Furthermore, the BSE mode has the advantage that it causes much less charging on insulating samples, as for the sample in this case. The finder structure (letters) can be used to find exactly the same area as in scanning probe microscopy and vice versa. Fig. 3b and c show SEM image and EDX aluminium K series maps respectively, of a similar area as in Fig. 2c and d. Fig. 3c clearly shows that aluminium is restricted only to coated areas. EDX mapping can be also used to distinguish between the coated and uncoated areas in case the average atomic number of film and sample is too similar for discrimination via BSE imaging. Note that bright features in Fig. 3b, correspond to ferroelectric domains which are visible in certain cases in SEM BSE imaging.

## Conclusions

We have shown that the marking technique is well suitable for imaging the same area with light microscopy, AFM and SEM. In principle, this marking technique can be used for many other microscopy techniques like confocal Raman microscopy or X-ray tomography with the only requirement that coated and uncoated areas need to be distinguishable. Such marked samples might also be particularly useful in junction with FIB sectioning, when e.g. a lamellar of specific pre-selected region needs to be obtained.

More than 500 areas with sizes of around  $15 \times 15 \mu\text{m}$  (larger sizes are also possible) can be marked distinguishably at one time which is especially important, if samples do not exhibit prominent features. Furthermore, many samples can be marked simultaneously which is advantageous for batch or high-throughput processing. The technique is inexpensive and convenient, e.g. it does not require expensive and time consuming FIB processing.

Best results are achieved, when the sample surface is flat and electron-beam evaporation with good line-of-sight deposition and relatively long sample to source distance is used, which results in sharper edges between coated and uncoated areas. The film material should be relatively hard which avoids problems with sample handling and imaging artifacts in AFM. In our case, aluminium (thickness approx. 60 nm) was well suitable for this purpose in contrast to gold.

### Acknowledgements

L. F. H acknowledges project funding by the European Commission through the ITN NANOMOTION (PITN-GA-2011-290158).

Processing of AFM-images was done using the free AFM software 'Gwyddion' (Nečas & Klapetek, 2012) for which excellent user support by D. Nečas is gratefully acknowledged.

### References

- Amos, W. B. & White, J. G. (2003) How the Confocal Laser Scanning Microscope entered Biological Research. *Biology of the Cell*, **95**, 335-342.
- Binnig, G., Quate, C. F. & Gerber, C. (1986) Atomic Force Microscope. *Phys. Rev. Lett.*, **56**, 930-933.
- Comyn, T. P., Stevenson, T. & Bell, A. J. (2004) Piezoelectric properties of BiFeO<sub>3</sub>-PbTiO<sub>3</sub> ceramics. In: *Applications of Ferroelectrics, 2004. ISAF-04. 2004 14th IEEE International Symposium*.
- Drexler, K. E. (1992) *Nanosystems: Molecular Machinery, Manufacturing, and Computation.*, John Wiley & Sons, New York.
- Fiebig, M. (2005) Revival of the magnetoelectric effect. *J. Phys. D: Appl. Phys.*, **38**, R123.
- Geim, A. K. & Novoselov, K. S. (2007) The rise of graphene. *Nat Mater*, **6**, 183-191.
- Giessibl, F. J. (2003) Advances in atomic force microscopy. *Rev. Mod. Phys.*, **75**, 949-983.
- Goodenough, J. B. & Park, K.-S. (2013) The Li-Ion Rechargeable Battery: A Perspective. *J. Am. Chem. Soc.*, **135**, 1167-1176.
- Henrichs, L. F., Bennett, J. & Bell, A. J. (2015) Choice of tip, signal stability, and practical aspects of piezoresponse-force-microscopy. *Rev. Sci. Instrum.*, **86**, 083707.

- Nečas, D. & Klapetek, P. (2012) Gwyddion: an open-source software for SPM data analysis. *Cent. Eur. J. Phys.*, **10**, 181-188.
- Rodriguez, B. J., Choudhury, S., Chu, Y. H., Bhattacharyya, A., Jesse, S., Seal, K., Baddorf, A. P., Ramesh, R., Chen, L.-Q. & Kalinin, S. V. (2009) Unraveling Deterministic Mesoscopic Polarization Switching Mechanisms: Spatially Resolved Studies of a Tilt Grain Boundary in Bismuth Ferrite. *Adv. Funct. Mater.*, **19**, 2053-2063.
- Sanborn, C. E. & Myers, S. A. (1991) Precision Tem Sample Preparation Using Focused Ion Beam Marking Strategies. *MRS Online Proceedings Library*, **254**.
- Soergel, E. (2011) Piezoresponse force microscopy (PFM). *J. Phys. D: Appl. Phys.*, **44**, 464003.
- Vernon-Parry, K. D. (2000) Scanning electron microscopy: an introduction. *III-Vs Review*, **13**, 40-44.